

Direction of Arrival Deception With Time-Modulated Scatterers

V. Kozlov¹, D. Vovchuk, *Graduate Student Member, IEEE*, and P. Ginzburg, *Member, IEEE*

Abstract—Modern radar systems can detect targets with high accuracy and are even able to classify them remotely. Their continuous advance is inevitably met with developing radar countermeasures, where passive radio-silent countermeasures begin to prevail over active jamming approaches. The direction of targets in respect to a radar system can be deduced from the correlation between the sampled phases in different antennas forming a receiving array. By breaking this coherent relationship, it is possible to cause the radar to estimate the wrong direction of arrival, deceiving it into concluding the object is elsewhere. A method for achieving this by controlling the reflected phase from a time-modulated scatterer is presented both theoretically and experimentally, showing suitability for implementation via time-dependent metasurfaces, supporting a semi-passive (battery-assisted) mode of operation. The method is also well suited for long range angular deception, complementing ‘cross-eye’ jamming techniques that are most effective at short ranges. We demonstrate control over the radar-perceived angular location of the static concealed target, with proven ability to steer the direction of arrival on demand by over 5 degrees away from its true angular position regardless of range. Remarkably, this new type of electronic countermeasure works better with increasing radar bandwidth, turning its strength into an exploitable weakness.

Index Terms—Radar countermeasures, electronic warfare, ECM, ECCM, time dependent metasurface covers, DOA deception.

I. INTRODUCTION

MODERN radar systems are an integral part of virtually any sensing application [1], [2], [3], [4], [5], [6], [7] and are expected to continue playing a major role in fused sensory networks. Their ubiquitous nature stems from their relatively low electromagnetic operational frequency which can penetrate fog, foliage, and other obstructions that complicate observation with optical and sonic devices alike. Yet it was exactly their tremendous success and widespread use that ushered a race for electronic countermeasures (ECM) to evade detection, which soon found themselves the target of countermeasures (ECCM) and so on in apparent perpetuity [8], [9], [10], [11], [12], [13]. Stealth technologies emerged

with the aim of minimizing the signatures of targets [14], [15], providing a passive solution to avoiding detection. But even for very absorbent materials and carefully crafted geometries, the standoff distance could only be reduced so much, with multi-static radars still posing a considerable challenge. To overcome these issues and to provide solutions in cases where radar scattering suppression strategies are not applicable, jamming measures keep developing and advancing. The traditional active jamming strategy relies on transmitting noise toward the radar to reduce its signal-to-noise ratio (SNR), diminishing the minimal range of detection at the expense of radio silence. Spoofing methods keep developing to supplement active jamming, with chaff decoys being the simplest example, designed to create false “ghost” targets on the screen of the investigating radar [16], [17], [18], [19], [20], [21], [22].

More advanced spoofing methods introduce repeaters that control the signatures on the reflected echoes, delaying them in time and imprinting false Doppler shifts which cause the radar to deduce the wrong trajectory and location of targets [23], [24], [25], [26]. So-called “Cross-eye” techniques, implemented by placing synchronized coherent repeaters at a distance from each other, deform the scattered phase fronts thus deceiving the radar into concluding the wrong angular location of the target at short ranges [27], [28], [29], [30], [31]. The main shortcoming of such methods stems from their inability to suppress the reflection from the target itself. Instead, the echo is superimposed with an amplified spoofed reflection from the repeater, thus attempting to cause the radar to track the more prominent ghost. It was not long for spoofing ECM to come under scrutiny from ECCM signal processing [32], [33], [34], severely challenging its effectiveness and continuing the apparently endless cycle of measures and countermeasures. Recently metamaterials and metasurfaces had been the focus of concentrated efforts to shape scattered waves from the targets themselves, enabling novel pathways to passive stealth capabilities [35], [36], [37].

Today, time-dependent control over the properties of metamaterials is introducing a new degree of freedom to the problem of detection evasion and radar deception. By carefully controlling the temporal scattering properties, it was shown possible to imprint arbitrary signatures on the backscattered reflections [38], [39], [40], [41], [42], [43]. These new designs promise to achieve similar performance to that of repeaters without suffering from their main drawback, the reliance on superimposed echoes, by effectively transforming the body of scatterers into a repeater in itself.

Manuscript received 13 January 2023; revised 12 April 2023; accepted 13 May 2023. Date of publication 23 May 2023; date of current version 7 June 2023. This work was supported in part by the Department of the Navy, Office of Naval Research Global, under ONRG Award N62909–21–1–2038. (*Corresponding author: V. Kozlov.*)

V. Kozlov and P. Ginzburg are with the School of Electrical Engineering, Tel Aviv University, Tel Aviv 69978, Israel (e-mail: vitaliko@mail.tau.ac.il).

D. Vovchuk is with the School of Electrical Engineering, Tel Aviv University, Tel Aviv 69978, Israel, and also with the Department of Radio Engineering and Information Security, Yuriy Fedkovych Chernivtsi National University, 58000 Chernivtsi, Ukraine.

Digital Object Identifier 10.1109/TRS.2023.3279238

2832-7357 © 2023 IEEE. Personal use is permitted, but republication/redistribution requires IEEE permission. See <https://www.ieee.org/publications/rights/index.html> for more information.

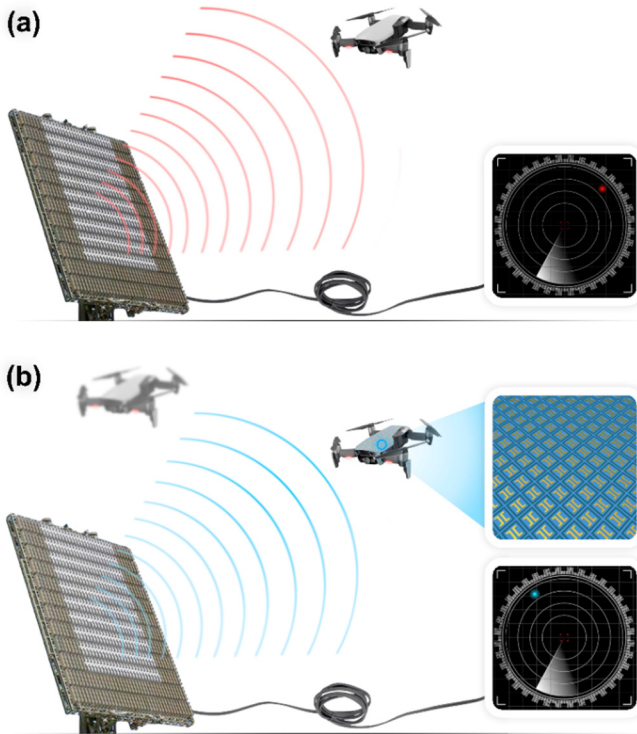


Fig. 1. Illustration of the proposed deception concept. A radar observing a drone with and without a metasurface cover (a) The drone without cover is detected. (b) Dynamic control of the scattering properties from the drone conceals its true angular location from the investigating radar.

While in the vast majority of deception scenarios range and Doppler are targeted, angular information is just as important for surveillance. However, direction of arrival (DOA) deception strategies are extremely challenging with only few ever reported in the literature [27], [28], [29], [30], [31]. The fundamental physical reason for this is that within a good approximation, most targets are essentially point like scatterers, generating a spherical-like outgoing wave. The wavefront at a large distance approaches a plane wave with respect to an investigating radar antenna array regardless of the geometric shape of the scattering body. To overcome this limitation, cross-eye jamming places two coherently synchronized repeaters at relatively large (greater than the wavelength) distance from each other. This solution becomes less effective for subwavelength scatterers, as can be the case for drones as an illustrative example. To achieve DOA deception for small targets an additional degree of freedom is required by employing time-dependent control over scattering properties of the reflecting target. Here a novel method for the DOA deception with time-dependent targets is proposed and demonstrated.

Fig.1 illustrates the scenario, where a target (a drone as an example) is shown with and without a time-modulated cloak while being observed by the same radar system. The concealed drone in Fig1(b) modulates the backscattered echoes phase in such a way that it appears to arrive from an entirely different direction than it truly is.

The manuscript is organized in the following way. First, a theoretical derivation of the proposed deception concept is performed. Then an experiment in the anechoic chamber

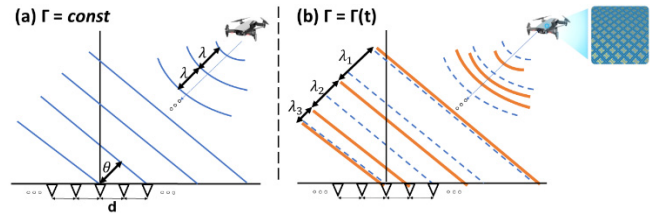


Fig. 2. The concept of direction of arrival deception by time-modulated scatterers. An array of receivers is observing (a) standard target, reflecting a plane wave towards the radar and (b) a time-modulated target, which controls its phase in such a way that the coherent relation between the phases of the receiving antennas is broken, concealing the true angular location of the drone.

is conducted, showing that it is indeed possible to deceive the radar into concluding the wrong direction of arrival on demand. The ‘Outlook and Conclusion’ section follows comparing the advantages and disadvantages of the method to cross-eye jamming.

II. THEORY

Consider a radar (ultra-wideband applications are outside of the scope of this manuscript) with a one-dimensional uniform array of antennas (non-uniform arrays will behave similarly) separated by a distance d , as depicted in Fig.2(a). For standard scattering objects, such as exemplified by the drone, the backscattered wave reaches the array at the far field, with the wavefront well approximated by a plane wave. The peaks of the impinging wave are marked by the blue equal-phase lines, separated by a distance comparable to the wavelength λ . This scenario is akin to the intuitive analogue in water waves, where direction of arrival can be determined by the phase delay between the rising time of floating buoys. If all the buoys rise at the same time, the wave must be arriving from the front ($\theta = 0$), while any other delay between the rise times has a one-to-one relation to the DOA. The complex field phasor at the location of the n^{th} ($n = 0, \pm 1, \pm 2 \dots$) antenna can be written as:

$$E_n \propto |\Gamma| e^{-j(nkd \sin(\theta) + \angle \Gamma)}, \quad (1)$$

where $\angle \Gamma$ is the phase of the reflection coefficient of the scatterer and $|\Gamma|$ is its amplitude, while $k = \frac{2\pi}{\lambda} = \frac{\omega}{c}$ is the free space wavenumber, ω the carrier frequency of the radar and c the speed of light.

The form of Eq. 1 suggests that detecting the direction of arrival is possible by Fourier transforming the vector of n samples and relating the largest output ‘frequency’ to the DOA. While this is the straightforward approach, extensive research was conducted in the field of signal processing, allowing to sample non-uniformly and sparsely, surpassing the resolution and accuracy achievable by the naïve approach by employing algorithms such as multi-signal classification (MUSIC) and others [44], [45]. It’s interesting to note that DOA estimation can be achieved with time-dependant metasurfaces that avoid the need for numerous receiving antennas and their associated costly radio frequency (RF) chains [46], [47], [48], [49], [50]. No matter what method of detection is used, Eq. 1 remains the basis for all, seeing as there is a deterministic correlation

between the phases in the different locations of the array-sampled space. To break this correlation, a time-modulated scatterer is required, one that can switch its reflected phase fast enough to decorrelate different receiving elements of the array, as shown in Fig. 2(b). The dashed blue lines represent the wavefronts reflected from the regular scatterer as in Fig. 2(a), while the orange lines represent the time-dependent wavefronts, with the peaks no longer having equal distance between them. In such a scenario the form of Eq. 1 remains, substituting $\Gamma \rightarrow \Gamma(t)$.

While fast random switching of the reflected phase will achieve the result of decorrelating the receivers, the required modulation will inevitably require fast changes on the order of the carrier frequency, which will place the reflected waveform well outside of the operational bandwidth of any reasonable radar system. While this can help concealing the target, the fast modulation will also cause the target to radiate by itself, making it visible to any passive radar devices. Instead, a slower harmonic modulation may be performed to retain radio silence:

$$\Gamma(t) = e^{-j\Omega t}, \quad (2)$$

where Ω can be positive or negative to reflect increasing or decreasing linear phase modulation respectively. Note that the amplitude of the reflection coefficient remains constant in time, as will be the case in the experiment ahead, where high-grade broadband phase-shifters have been used. In case of narrow band resonant metasurfaces, the amplitude can become frequency-dependent. Substituting Eq. 2 into Eq. 1 and considering the phase difference between adjacent antennas leads to:

$$\Delta\phi = \left(1 + \frac{\Omega}{\omega}\right)kd\text{Sin}(\theta). \quad (3)$$

Eq. 3 reduces to the standard phase difference in classical linear antenna arrays when $\Omega = 0$, allowing to derive the relation between the real DOA θ_{real} and that which will be estimated by an unsuspecting algorithm (please see the discussion ahead about this assumption):

$$\begin{aligned} \theta_{estimated} &= \text{Sin}^{-1}\left(\frac{\Delta\phi}{kd}\right) \\ &= \text{Sin}^{-1}\left(\left(1 + \frac{\Omega}{\omega}\right)\text{Sin}(\theta_{real})\right). \end{aligned} \quad (4)$$

Eq. 4 clearly suggests that a controllable error could be introduced into the DOA estimation of the investigating radar, which will depend solely on the modulation frequency Ω of the reflecting time-modulated target. It should be noted that considerable modulation is required in this case. Performing a linear approximation of Eq. 4, under the assumption of near normal incidence ($\theta_{real} \ll 1[\text{rad}]$ and even for larger angles as a reasonable approximation) results in a simple expression for the DOA error:

$$\Delta\theta = |\theta_{estimated} - \theta_{real}| \approx \frac{\Omega}{\omega}\theta_{real}, \quad (5)$$

suggesting that exceeding an error by a few degrees can require the modulation frequency to be above 5% of the carrier wave. Since 10% bandwidth around the carrier is fairly common for

radar systems (e.g., L-band airport surveillance), the proposed method is practical in real life scenarios. The final point to consider for real radar systems is the effect of this deception on the Doppler velocity perceived by the radar.

At first glance, it might appear that the high frequency shift Ω caused by the harmonic modulation in Eq.2 can be used to reveal that the proposed DOA deception method is being used as a countermeasure. Observing high Doppler shifts, which cannot be related to velocities of realistic objects in a scene, arouse suspicion. However, since the frequency shift of the carrier is still within the bandwidth of the radar, it will be folded by the sampler into the Doppler domain defined by its pulse repetition frequency (PRF). By choosing the modulation frequency Ω as a (large) even integer of the PRF, the Doppler frequency can be made to vanish entirely, causing the target to appear static. By choosing some other modulation frequency the time modulated scatterer can be made to appear at arbitrary Doppler velocity. Note that in the experiment shown ahead the modulation frequencies are in the range of tens of MHz while Doppler velocities are orders of magnitude lower.

While using staggered pulses (alternating PRF sequences) could help resolve some of the Doppler ambiguity, resolving the very large frequency shift proposed here (above 5% from the carrier frequency) would require extreme alteration of the PRF, which is hard to implement in any practical radar system, making the proposed DOA deception method suitable for integration with Doppler deception techniques [38], [39], [40], [41], [42], [43]. As a side note, it is possible to counter the proposed deception technique by implementing an analogue frequency measurement block that will correctly deduce that a large carrier frequency shift is occurring. Finally, the proposed shift will inevitably cause some of the radar waveform to remain outside of the radar's bandwidth, meaning that matched filters will lose some SNR as well as add deformation to the output. The larger the frequency shift Ω is, the more distortion will be inflicted on the matched output.

However, bandwidth is only a figure of merit that promises some acceptable attenuation in that band, it does not completely filter out nearby frequencies, suggesting it is reasonable to expect that even a large shift by an amount of half the bandwidth ($\Omega = \frac{B}{2}$) would still be detectable. This allows to place an upper bound on the DOA error that can be achieved using the proposed method:

$$\Delta\theta_{max} \approx \frac{B}{2\omega}\theta_{real}. \quad (6)$$

III. EXPERIMENT

To validate the theoretical results described above, an experiment was conducted in the anechoic chamber as shown in Fig. 3. A continuous wave (CW) radar was assembled with the carrier frequency of 820MHz, consisting of a transmitting UHF log-periodic antenna (CLP5130-2) directed at the time-modulated scatterer, as well as a 4-element uniformly spaced antenna array ($d = \frac{\lambda}{2} = 183 \text{ mm}$) that recorded the reflected echoes. Signals on the two central antennas were directly sampled by a scope (Keysight DSOX3104T) while

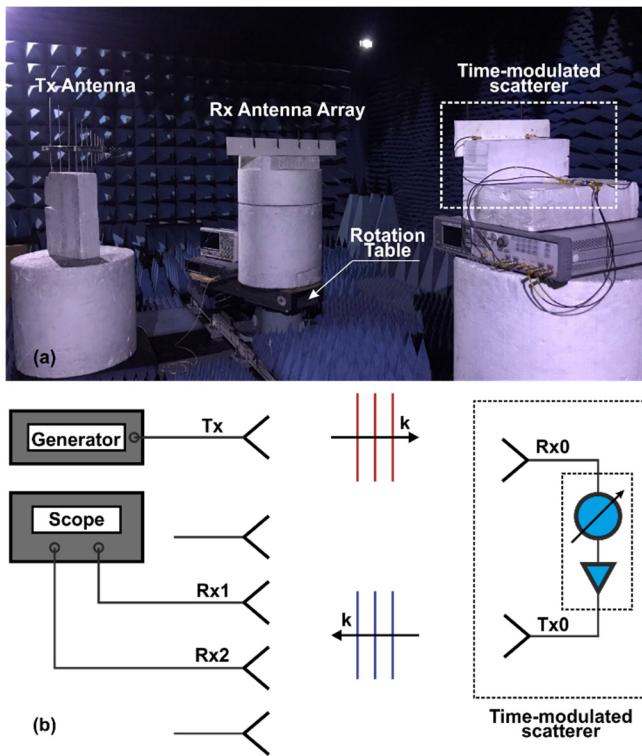


Fig. 3. The experimental setup in the anechoic chamber, a CW radar is interrogating the time-modulated scatterer. The DOA system is realized with two antennas - a transmitting log-periodic antenna and receiving a 4-element uniform antenna array. The schematic inset shows the electronics of the scatterer, comprising identical receive and transmit horn antennas. The inset shows the schematic makeup of the scatterer, comprised of a delay line, bias-controlled phase shifter, and amplifier, which allow for dynamic arbitrary reflected phase control.

the peripheral two antennas located on the sides of the array were loaded with 50 Ohm terminations for better matching of the receivers. The time-modulated scatterer that is shown in Fig. 3 was constructed from a pair of identical antennas, one receiving and the other transmitting, with a phase shifter placed in between as seen in the inset to Fig. 3.

The phase shifter was controlled by an RF vector modulator (AD8340), capable of arbitrary dynamic phase control over more than 60MHz bandwidth, which was followed by an amplifying stage to compensate for losses. The control over the phase of the RF vector modulator was performed with an arbitrary function generator (Keysight 81160A), which was configured to create harmonic modulation as in Eq. 2. The receiving array was placed on a rotating table, allowing to control the true DOA of the target. It is worth noting that a single impedance-modulated scatterer (without an amplifying unit) can be used. Here we used its replica to reduce the design complexity and also to avoid a need to send high-power signals, which are restricted by laboratory and regulatory arrangements.

The experimental setup was first calibrated by recording the phases at the receivers for a forward-facing scatterer ($\theta_{real} = 0$) with its modulation frequency set to 0Hz (no modulation). In this case, the phase difference between the receivers is expected to be 0 for perfectly calibrated instrumentation, however, the various lengths of connecting cables and other

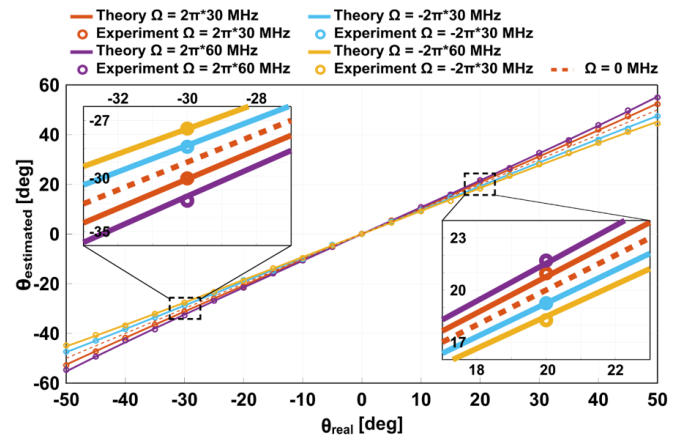


Fig. 4. Demonstration of control over the perceived direction of arrival of the time-modulated target. By controlling the modulation frequency of the reflected phase from the object, it may appear to the radar in a different direction than it truly is, with increasing modulation frequency and true angular location increasing the error. Insets zoom in on regions of interest.

equipment in the receiver can cause a phase shift between the channels. Calibration is therefore simply performed by subtracting these measured values from all subsequent measurements at each antenna ($\phi \rightarrow \phi - \phi_{calib}$). The experiment was conducted by rotating the receiving array by 10-degree steps from -50 to 50 degrees, estimating the DOA using the calibration and Eq. 4 (substituting $\Omega = 0$, which corresponds to an unsuspecting radar system anticipating echoes to not be significantly shifted in frequency).

The experiment was repeated by performing positive and negative modulations of 30 and 60 MHz, where the sign corresponds to increasing or decreasing phase modulation as in Eq. 2. The results are shown in Fig. 4, showing excellent agreement between the theoretical prediction in Eq. 4 and experiment. Over 5 degrees of DOA at the edges of the sampled parameters ($\Omega = \pm 60 \text{ MHz}$, $\theta_{real} = \pm 50 \text{ [deg]}$). Indeed, a linear relationship can be observed between the real and estimated DOA, with the slope proportional to the modulation frequency, demonstrating steerability of the perceived DOA by modulation of the time dependent scatterer.

IV. OUTLOOK AND CONCLUSION

A novel direction of arrival deception method was demonstrated, enabled by dynamic control over the scattering properties of the time-dependent target. In particular, upwards of 5 degrees of steerable angular errors were demonstrated for a radar system, possessing a relatively high yet practical bandwidth of about 10% around its central carrier frequency (note that while the effectiveness of the method increases with bandwidth, there is no objective threshold).

While cross-eye jamming successfully deceives DOA at a short distance, the proposed method can work well at an arbitrary range to the target radar, supporting the use of both methods in a complementary fashion. Additional advantages of the method include complete spherical coverage, which does not require any knowledge about the deceived radar location or modes of operation (aside from operational bandwidth). Seeing as this method is particularly appealing for integration

with metasurface coatings, we expect future implementations of such covers to be designed based on the principles outlined in the presented method, where phase control will be achieved on demand. Additional consideration should be taken when concealing large objects, ensuring the scattered field in the desired direction (location of the investigating radar) is correctly added coherently from all the various scattering centers. The limitations of the method are primarily dependent on the bandwidth of the observing radar. Remarkably, the more broadband a radar is, the more susceptible it will be to such deception, as shown in Eq. 6. While the method does not require knowledge of the direction of the interrogating radar to counteract it, its angular position will determine how much error will be introduced, as described by Eq. 5. Additional considerations are the PRF of the investigating system, which are frequently staggered (alternate) in order to remove Doppler and range ambiguities. Staggered pulses reflected from such a time-dependent scatterer will cause alternating Doppler frequencies associated with the target, however, it will likely be resolved by the system simply as the closest reasonable one above the Nyquist velocity. While this can still make the target appear somewhat fast to the radar, this can serve to further confuse its tracker, which will struggle to make sense of the discrepancy between the fast expected velocity and the much slower actual range rate of the target.

The reported method can be implemented alongside previously reported deceptions with time-dependent scatterer, allowing to present arbitrary range and velocity to the interrogating radar, accounting for the entirety of the available degrees of freedom measurable by such systems. It is also worth noting that deceiving multiple parameters simultaneously, even if a real object is not replaced by a coherent ghost target, makes ECCM algorithms face severe challenges, especially in cases where real-time operation is demanded.

REFERENCES

- [1] R. Klemm, H. Griffiths, and W. Koch, *Novel Radar Techniques and Applications*, vol. 2. Institution of Engineering and Technology, 2017.
- [2] A. F. M. Mahfouz, "See-through-wall imaging using ultra wideband pulse systems," in *Proc. 34th Appl. Imag. Pattern Recognit. Workshop (AIPR)*, 2005, pp. 48–53, doi: [10.1109/AIPR.2005.40](https://doi.org/10.1109/AIPR.2005.40).
- [3] J. S. Lee, C. Nguyen, and T. Scullion, "A novel, compact, low-cost, impulse ground-penetrating radar for nondestructive evaluation of pavements," *IEEE Trans. Instrum. Meas.*, vol. 53, no. 6, pp. 1502–1509, Dec. 2004, doi: [10.1109/TIM.2004.827308](https://doi.org/10.1109/TIM.2004.827308).
- [4] M. Murad, J. Nickolaou, G. Raz, J. S. Colburn, and K. Geary, "Next generation short range radar (SRR) for automotive applications," in *Proc. IEEE Radar Conf.*, May 2012, pp. 214–219, doi: [10.1109/RADAR.2012.6212139](https://doi.org/10.1109/RADAR.2012.6212139).
- [5] P. Van Dorp and F. C. A. Groen, "Human walking estimation with radar," *IEE Proc., Radar, Sonar Navigat.*, vol. 150, no. 5, pp. 356–366, Oct. 2003, doi: [10.1049/IP-RSN:20030568](https://doi.org/10.1049/IP-RSN:20030568).
- [6] C. Gu, C. Li, J. Lin, J. Long, J. Huangfu, and L. Ran, "Instrument-based noncontact Doppler radar vital sign detection system using heterodyne digital quadrature demodulation architecture," *IEEE Trans. Instrum. Meas.*, vol. 59, no. 6, pp. 1580–1588, Jun. 2010, doi: [10.1109/TIM.2009.2028208](https://doi.org/10.1109/TIM.2009.2028208).
- [7] V. Kozlov, D. Vovchuk, S. Kosulnikov, D. Filonov, and P. Ginzburg, "Micro-Doppler signatures of subwavelength nonrigid bodies in motion," *Phys. Rev. B, Condens. Matter*, vol. 104, no. 5, Aug. 2021, Art. no. 054307, doi: [10.1103/PHYSREVB.104.054307](https://doi.org/10.1103/PHYSREVB.104.054307).
- [8] P. M. Grant and J. H. Collins, "Introduction to electronic warfare," *IEE Proc. F, Commun. Radar Signal Process.*, vol. 129, no. 3, pp. 113–132, 1982, doi: [10.1049/ip-f-1.1982.0020](https://doi.org/10.1049/ip-f-1.1982.0020).
- [9] L. Neng-Jing and Z. Yi-Ting, "A survey of radar ECM and ECCM," *IEEE Trans. Aerosp. Electron. Syst.*, vol. 31, no. 3, pp. 1110–1120, Jul. 1995, doi: [10.1109/7.395232](https://doi.org/10.1109/7.395232).
- [10] F. A. Butt, I. H. Naqvi, and A. I. Najam, "Radar ECCM against deception jamming: A novel approach using bi-static and mono-static radars," in *Proc. 15th Int. Multitopic Conf. (INMIC)*, Dec. 2012, pp. 137–141, doi: [10.1109/INMIC.2012.6511482](https://doi.org/10.1109/INMIC.2012.6511482).
- [11] D. J. Bachmann, R. J. Evans, and B. Moran, "Game theoretic analysis of adaptive radar jamming," *IEEE Trans. Aerosp. Electron. Syst.*, vol. 47, no. 2, pp. 1081–1100, Apr. 2011, doi: [10.1109/TAES.2011.5751244](https://doi.org/10.1109/TAES.2011.5751244).
- [12] G. Frazer, A. Balleri, and G. S. Jacob, "Deception jamming against Doppler beam sharpening radars," in *Proc. IEEE Radar Conf. (Radar-Conf)*, Apr. 2019, pp. 1–6, doi: [10.1109/RADAR.2019.8835600](https://doi.org/10.1109/RADAR.2019.8835600).
- [13] R. Chauhan, "A platform for false data injection in frequency modulated continuous wave radar," Utah State Univ., Logan, UT, USA, 2014.
- [14] G. A. Rao and S. P. Mahulikar, "Integrated review of stealth technology and its role in airpower," *Aeronaut. J.*, vol. 106, no. 1066, pp. 629–642, Dec. 2002, doi: [10.1017/S0001924000011702](https://doi.org/10.1017/S0001924000011702).
- [15] W. F. Bahret, "The beginnings of stealth technology," *IEEE Trans. Aerosp. Electron. Syst.*, vol. AES-29, no. 4, pp. 1377–1385, Oct. 1970.
- [16] C. H. Cheng and J. Tsui, "An introduction to electronic warfare; from the first jamming to machine learning techniques," in *An Introduction to Electronic Warfare: From the First Jamming to Machine Learning Techniques*. Denmark: River Publishers, Jan. 2021, pp. 1–167.
- [17] S. Kosulnikov et al., "Circular wire-bundle superscatterer," *J. Quant. Spectrosc. Radiat. Transf.*, vol. 279, Mar. 2022, Art. no. 108065, doi: [10.1016/j.jqsrt.2022.108065](https://doi.org/10.1016/j.jqsrt.2022.108065).
- [18] D. Dobrykh et al., "Multipole engineering for enhanced backscattering modulation," *Phys. Rev. B, Condens. Matter*, vol. 102, no. 19, Nov. 2020, Art. no. 195129, doi: [10.1103/PHYSREVB.102.195129](https://doi.org/10.1103/PHYSREVB.102.195129).
- [19] D. Filonov, A. Shmidt, A. Boag, and P. Ginzburg, "Artificial localized magnon resonances in subwavelength meta-particles," *Appl. Phys. Lett.*, vol. 113, no. 12, Sep. 2018, Art. no. 123505, doi: [10.1063/1.5047445](https://doi.org/10.1063/1.5047445).
- [20] K. Grotov et al., "Genetically designed wire bundle superscatterers," *IEEE Trans. Antennas Propag.*, vol. 70, no. 10, pp. 9621–9629, Oct. 2022, doi: [10.1109/TAP.2022.3177531](https://doi.org/10.1109/TAP.2022.3177531).
- [21] A. Mikhailovskaya et al., "Superradiant scattering limit for arrays of subwavelength scatterers," *Phys. Rev. Appl.*, vol. 18, no. 5, Nov. 2022, Art. no. 054063, doi: [10.1103/PhysRevApplied.18.054063](https://doi.org/10.1103/PhysRevApplied.18.054063).
- [22] D. Vovchuk, S. Kosulnikov, R. E. Noskov, and P. Ginzburg, "Wire resonator as a broadband Huygens superscatterer," *Phys. Rev. B, Condens. Matter*, vol. 102, no. 9, Sep. 2020, Art. no. 094304, doi: [10.1103/PhysRevB.102.094304](https://doi.org/10.1103/PhysRevB.102.094304).
- [23] R. Komissarov, S. Vaisman, and A. Wool, "Spoofing attacks against vehicular FMCW radar," *J. Cryptograph. Eng.*, vol. 2023, pp. 1–12, May 2023, doi: [10.1007/S13389-023-00321-5](https://doi.org/10.1007/S13389-023-00321-5).
- [24] A. Lazaro, A. Porcel, M. Lazaro, R. Villarino, and D. Girbau, "Spoofing attacks on FMCW radars with low-cost backscatter tags," *Sensors*, vol. 22, no. 6, p. 2145, Mar. 2022, doi: [10.3390/S22062145](https://doi.org/10.3390/S22062145).
- [25] D. Feng, L. Xu, X. Pan, and X. Wang, "Jamming wideband radar using interrupted-sampling repeater," *IEEE Trans. Aerosp. Electron. Syst.*, vol. 53, no. 3, pp. 1341–1354, Jun. 2017, doi: [10.1109/TAES.2017.2670958](https://doi.org/10.1109/TAES.2017.2670958).
- [26] D. H. A. Maithripala and S. Jayasuriya, "Radar deception through phantom track generation," in *Proc. Amer. Control Conf.*, vol. 6, 2005, pp. 4102–4106, doi: [10.1109/ACC.2005.1470620](https://doi.org/10.1109/ACC.2005.1470620).
- [27] F. Neri, *Introduction to Electronic Defense Systems*, 2001, p. 622. Accessed: Apr. 11, 2023. [Online]. Available: https://books.google.com/books/about/Introduction_to_Electronic_Defense_Systeme.html?hl=uk&id=SoR0IEoGz5EC
- [28] W. P. Warren and P. Du Plessis. (Jun. 2010). *A Comprehensive Investigation of Retrodirective Cross-Eye Jamming*. Accessed: Apr. 11, 2023. [Online]. Available: <https://repository.up.ac.za/handle/2263/25480>
- [29] F. Pieterse and W. P. D. Plessis, "Implementation and testing of a retrodirective cross-eye jammer," *IEEE Trans. Aerosp. Electron. Syst.*, vol. 58, no. 5, pp. 4486–4494, Oct. 2022, doi: [10.1109/TAES.2022.3164017](https://doi.org/10.1109/TAES.2022.3164017).
- [30] W. P. du Plessis, J. W. Odendaal, and J. Joubert, "Experimental simulation of retrodirective cross-eye jamming," *IEEE Trans. Aerosp. Electron. Syst.*, vol. 47, no. 1, pp. 734–740, Jan. 2011, doi: [10.1109/TAES.2011.5705704](https://doi.org/10.1109/TAES.2011.5705704).
- [31] J.-A. Kim and J.-H. Lee, "Performance degradation in cross-eye jamming due to amplitude/phase instability between jammer antennas," *Sensors*, vol. 21, no. 15, p. 5027, Jul. 2021, doi: [10.3390/S21155027](https://doi.org/10.3390/S21155027).

- [32] J. Zhang, D. Zhu, and G. Zhang, "New antivelocety deception jamming technique using pulses with adaptive initial phases," *IEEE Trans. Aerosp. Electron. Syst.*, vol. 49, no. 2, pp. 1290–1300, Apr. 2013, doi: [10.1109/TAES.2013.6494414](https://doi.org/10.1109/TAES.2013.6494414).
- [33] Z. Liu, J. Sui, Z. Wei, and X. Li, "A sparse-driven anti-velocity deception jamming strategy based on pulse-Doppler radar with random pulse initial phases," *Sensors*, vol. 18, no. 4, p. 1249, Apr. 2018, doi: [10.3390/S18041249](https://doi.org/10.3390/S18041249).
- [34] C. Zhou, Z. B. Zhu, and Z. Y. Tang, "A novel waveform design method for shift-frequency jamming confirmation," *Int. J. Antennas Propag.*, vol. 2018, Jul. 2018, Art. no. 1569590, doi: [10.1155/2018/1569590](https://doi.org/10.1155/2018/1569590).
- [35] D. Schurig et al., "Metamaterial electromagnetic cloak at microwave frequencies," *Science*, vol. 314, no. 5801, pp. 977–980, Nov. 2006, doi: [10.1126/science.1133628](https://doi.org/10.1126/science.1133628).
- [36] P. Alitalo and S. Tretyakov, "Electromagnetic cloaking with metamaterials," *Mater. Today*, vol. 12, no. 3, pp. 22–29, Mar. 2009, doi: [10.1016/S1369-7021\(09\)70072-0](https://doi.org/10.1016/S1369-7021(09)70072-0).
- [37] R. Fleury and A. Alù, "Cloaking and invisibility: A review," in *Forum for Electromagnetic Research Methods and Application Technologies (FERMAT)*, vol. 1, no. 9. Laboratory of Wave Engineering, EPFL, 2014.
- [38] V. Kozlov, D. Vovchuk, and P. Ginzburg, "Broadband radar invisibility with time-dependent metasurfaces," *Sci. Rep.*, vol. 11, no. 1, pp. 1–11, Jul. 2021, doi: [10.1038/s41598-021-93600-2](https://doi.org/10.1038/s41598-021-93600-2).
- [39] X. G. Zhang et al., "Smart Doppler cloak operating in broad band and full polarizations," *Adv. Mater.*, vol. 33, no. 17, Apr. 2021, Art. no. 2007966, doi: [10.1002/ADMA.202007966](https://doi.org/10.1002/ADMA.202007966).
- [40] B. Liu, Y. He, S. W. Wong, and Y. Li, "Experimental demonstration of a time-domain digital-coding metasurface for a Doppler cloak," *Opt. Exp.*, vol. 29, no. 2, pp. 740–750, Jan. 2021, doi: [10.1364/OE.414408](https://doi.org/10.1364/OE.414408).
- [41] B. Liu, H. Giddens, Y. Li, Y. He, S.-W. Wong, and Y. Hao, "Design and experimental demonstration of Doppler cloak from spatiotemporally modulated metamaterials based on rotational Doppler effect," *Opt. Exp.*, vol. 28, no. 3, p. 3745, Feb. 2020, doi: [10.1364/oe.382700](https://doi.org/10.1364/oe.382700).
- [42] D. Ramaccia, D. L. Sounas, A. Alù, A. Toscano, and F. Bilotti, "Phase-induced frequency conversion and Doppler effect with time-modulated metasurfaces," *IEEE Trans. Antennas Propag.*, vol. 68, no. 3, pp. 1607–1617, Mar. 2020, doi: [10.1109/TAP.2019.2952469](https://doi.org/10.1109/TAP.2019.2952469).
- [43] V. Kozlov, D. Vovchuk, and P. Ginzburg, "Radar range deception with time-modulated scatterers," *IEEE Trans. Antennas Propag.*, vol. 71, no. 5, pp. 4486–4491, May 2023, doi: [10.1109/TAP.2023.3255108](https://doi.org/10.1109/TAP.2023.3255108).
- [44] T. E. Tuncer and B. Friedlander, Eds., *Classical and Modern Direction-of-Arrival Estimation*, 1st ed. New York, NY, USA: Academic, 2009.
- [45] H. L. Van Trees, *Optimum Array Processing*. Hoboken, NJ, USA: Wiley, Mar. 2002, doi: [10.1002/0471221104](https://doi.org/10.1002/0471221104).
- [46] X. Wang and C. Caloz, "Direction-of-arrival (DOA) estimation based on spacetime-modulated metasurface," in *Proc. IEEE Int. Symp. Antennas Propag., USNC-URSI Radio Sci. Meeting*, Jul. 2019, pp. 1613–1614, doi: [10.1109/APUSNCURSINRSM.2019.8888325](https://doi.org/10.1109/APUSNCURSINRSM.2019.8888325).
- [47] X. Fang et al., "Accurate direction-of-arrival estimation method based on space-time modulated metasurface," *IEEE Trans. Antennas Propag.*, vol. 70, no. 11, pp. 10951–10964, Nov. 2022, doi: [10.1109/TAP.2022.3184556](https://doi.org/10.1109/TAP.2022.3184556).
- [48] Q. Y. Zhou et al., "Two-dimensional direction-of-arrival estimation based on time-domain-coding digital metasurface," *Appl. Phys. Lett.*, vol. 121, no. 18, Oct. 2022, Art. no. 181702, doi: [10.1063/5.0124291](https://doi.org/10.1063/5.0124291).
- [49] T. V. Hoang, V. Fusco, M. A. B. Abbasi, and O. Yurduseven, "Single-pixel polarimetric direction of arrival estimation using programmable coding metasurface aperture," *Sci. Rep.*, vol. 11, no. 1, pp. 1–17, Dec. 2021, doi: [10.1038/s41598-021-03228-5](https://doi.org/10.1038/s41598-021-03228-5).
- [50] D. Vovchuk, M. Khobzei, D. Filonov, and P. Ginzburg, "Naked eye direction of arrival estimation with a Fresnel lens," *Sci. Rep.*, vol. 12, no. 1, pp. 1–10, Feb. 2022, doi: [10.1038/s41598-022-06480-5](https://doi.org/10.1038/s41598-022-06480-5).



V. Kozlov received the B.Sc. degree in physics and B.Sc. degree in electrical and electronics engineering and the M.Sc. degree from Tel Aviv University, Tel Aviv, Israel, in 2015 and 2017, respectively, where he is currently pursuing the Ph.D. degree.

His fields of interest focus on time dependent scattering phenomena, dynamic metasurfaces and their application towards radar and communication.



D. Vovchuk (Graduate Student Member, IEEE) received the B.Sc. and M.Sc. degrees from Yuriy Fedkovych Chernivtsi National University, Ukraine.

He has been performing his research at the School of Electrical Engineering of Tel Aviv University, Israel, from 2019. The fields of interests: radars, superscattering and superdirectivity, micro-doppler, deterministic chaos for communication systems.



P. Ginzburg (Member, IEEE) received the Ph.D. degree from Technion in 2011.

He is an Associate Professor at Tel Aviv University. He is a former EPSRC Research Fellow, International Newton Research Fellow, and Rothschild Fellow at King's College London. He is the Head of 'Dynamics of Nanostructures' Laboratory, encompassing theoretical group, optical spectroscopy, and radio waves labs. The Laboratory runs multidisciplinary research in the field of Biophotonics, Quantum Mechanics, Nano-plasmonics and

Metamaterials, and Radio Physics.